Comparison of frequency constants for $r/s = 4/3$

Case	No.	Exact	Frequency constant 10 d.o.f.	4 d.o.f.	20 d.o.f.	4 d.o.f.
1) Cantilever beam	1	3.52	3.52		3.52	
	2	22.03	22.51		22.07	
	3	61.70	64.98		62.77	
2) Simply-supported beam	1	9.87	9.87		9.87	
	2	39.48	39.54		39.92	
	3	88.82	89.63		88.87	
3) Free-free beam	1	22.37			22.42	
	2	61.67			61.91	
	3	120.91			123.60	

Here η is a column vector of generalized coordinates. Then the reduced eigenvalue problem is

$$\tilde{D}\eta = \ddot{\eta} \tag{5}$$

where

$$\underset{(r\times r)}{\tilde{D}} = \underset{(r\times r)}{[T^t \ K \ T]^{-1}} \cdot \underset{(r\times r)}{[T^t \ M \ T]} \tag{6}$$

This is a drastically reduced problem not requiring significant inversions if the condensation is effective by the criterion described above.

For free-free vibration, rigid body modes A_0 can be adjoined to T as

$$q = [A_0 \quad T]\begin{Bmatrix}\eta_0\\ \eta\end{Bmatrix} \tag{7}$$

where A_0 is a rectangular matrix of rigid body modes.[5]

Operation of the modified transformation matrix on K and M gives

$$\tilde{D} = [T^t \ K \ T]^{-1}\left[T^t \ M \ T - [T^t \ M \ A_0]\times [A_0^t \ M \ A_0]^{-1}[A_0^t \ M \ T]\right]$$

with the relation

$$\eta_0 = -[A_0^t \ M \ A_0]^{-1}[A_0^t \ M \ T]\{\eta\} \tag{8}$$

Thus, the eigenvalue problem is reduced from n to $r \ll n$.

Unlike "relaxation" methods, no assumption of zero loads at condensed freedoms is implied. The major computational effort is already contained within the decomposition necessary for static analysis, and therefore should be less than for other condensation schemes.

Examples

To demonstrate the potential of this approach a few simple computations were made using finite beam elements: 1) a cantilever beam—5, 10 elements, 2) a simply supported beam—5, 10 elements, and 3) a free-free beam—10 elements, with condensation to a 4×4 matrix. Table 1 shows the very good agreement compared with the exact results.

Conclusions

The method suggests improvement in economy with reliability in both eigenvalue and eigenvector results. The comparative closeness of the ratio $r \div s$ to unity confirms a combination of efficiency with physical and mathematical appropriateness. The arbitrariness of choice of condensed freedoms is eliminated, with only the number of freedoms to be retained to be decided.

In a highly complex structural system, selection of the deformation vectors can be supplemented by an automated linear independency criterion which has been utilized in the example quoted. It would seem practical to extend the basic idea to include a rational approach to the handling of substructured problems. Thus, boundary choices might be automated and the over-all problem optimized.

References

[1] Argyris, J. H., "Some Results on the Free-Free Oscillations of Aircraft Type Structures," *Revue Francaise de Mecanique*, No. 15, 1965, pp. 59–73.

[2] Guyan, R. J., "Reduction of Stiffness and Mass Matrices," *AIAA Journal*, Vol. 3, No. 2, Feb. 1965, pp. 380.

[3] Ojalvo, I. V. and Newman, M., "Vibration Modes of Large Structures by an Automatic Matrix-Reduction Method," *AIAA Journal*, Vol. 8, No. 7, July 1970, pp. 1234–1239.

[4] Lanczos, C., "An Iterative Method for the Solution of the Eigenvalue Problem of Linear Differential and Integral Operators," *Journal of Research*, Vol. 45, National Bureau of Standards, 1950, pp. 255–282.

[5] Argyris, J. H. and Kelsey, S., *Modern Fuselage Analysis and the Elastic Aircraft*, Butterworth, London, 1963, pp. 93–96.

Wind-Tunnel Magnus Testing of a Canted Fin or Self-Rotating Configuration

ANDERS S. PLATOU*

U.S. Army Ballistic Research Laboratories, Aberdeen Proving Ground, Md.

Nomenclature

d = body diameter
m_p = yaw couple due to opposing forces $N \sin\varepsilon$ and N_p
p = spin in rad/sec
u = air velocity
C_n = measured yawing moment coefficient
C_N = normal force coefficient on the configuration $(N/\frac{1}{2}\rho u^2 S)$
C_{N_p} = Magnus force coefficient $= [N_p/\frac{1}{2}\rho u^2 S(pd/u)]$
C_Y = measured side force coefficient
N = normal force
N_p = Magnus force
N_s = normal force due to an angle of yaw
S = cross-sectional body area $= \pi d^2/4$
α = indicated angle of attack
β = angle of yaw at zero indicated angle of attack
ε = angle of roll of true angle-of-attack plane
ρ = air density
l = distance between $N \sin\varepsilon$ and N_p
l_F = Magnus force c.p. to c.g. distance
l_N = normal force c.p. to c.g. distance

Introduction

RECENT studies have shown that Magnus wind-tunne measurements on canted fin or self-rotating configuration contain a normal force interaction term due to the inclinatio of the pitch plane with respect to the balance measurin directions. This interaction term is not the standard balanc interaction problem, but insteady requires that the amount o pitch plane inclination be calculated from zero spin pitch an Magnus data. It is also possible in the case discussed in thi paper to make the correction after assuming the Magnus forc center of pressure location. The interaction term can be suffi

Received February 2, 1972; revision received February 29, 1972.

Index categories: Uncontrolled Rocket and Missile Dynamic Rocket Vehicle Aerodynamics.

* Aerospace Engineer.

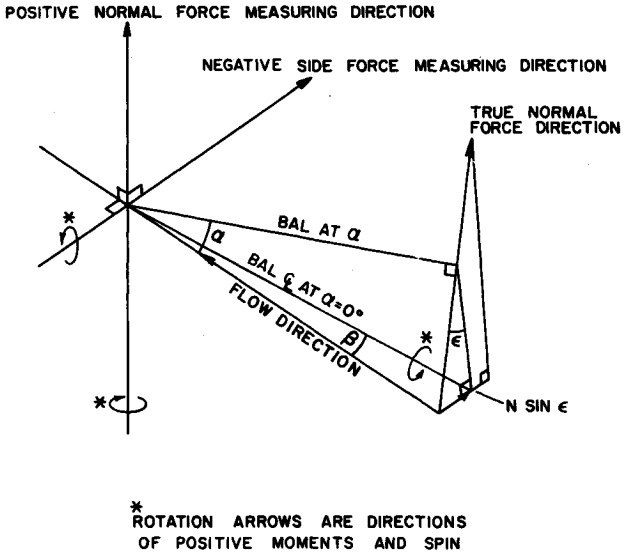

Fig. 1 The geometry involved in measuring magnus forces.

ciently large, so that if not eliminated, it will completely mask the Magnus force and moment.

Normal Force Interaction Error

In order to explain the interaction error let us assume that we have a test section tunnel flow which is exactly horizontal and contains no variation of flow inclination or Mach number in the test region. Let us also assume that the strain gage balance has no interaction terms and that the normal force or pitching moment measuring plane is exactly vertical and that the side force and moment measuring plane is exactly horizontal. All appears to be ideal except for one item. When installed in the test section at zero indicated angle of attack, the model and balance are at an angle of yaw β, Fig. 1. The side force developed on the configuration at zero spin is then

$$N_s = C_{N\alpha}\tfrac{1}{2}\rho u^2\beta(\pi d^2/4) \tag{1}$$

or the true angle-of-attack plane can be considered as being horizontal even though the indicated angle of attack is zero. As the indicated angle of attack is changed the true angle-of-attack plane will rotate such that

$$\sin\varepsilon = \tan\beta/\sin\alpha \tag{2}$$

The normal force which acts in the true angle-of-attack plane will then have a component acting in the side force measuring direction such that $N_s = N\sin\varepsilon$. If one does not measure N_s at zero spin and at each angle of attack, its value is included in the data obtained while the model is spinning.

Normally, since the zero spin data are difficult or impossible to obtain on a self-rotating configuration, experimenters have tended to present the results of the spinning data at angle of attack minus the spin data at zero angle of attack. These data still contain the normal force interaction term and really present the $pd/u\,C_{Np} - C_{N\alpha}\sin\varepsilon$.

A striking example of this error is shown in Ref. 1. The side force and moment acting on the canted fin configuration of Ref. 1 is presented in Fig. 2. The force is negative at low angles of attack, but becomes positive above 6° angle of attack. The moment, on the other hand, is positive at low angles, remains positive as the force crosses over at 6° and does not become negative until higher angles are reached. The existence of a moment at zero force is indicative of a couple and is due to the normal force interaction term ($N\sin\varepsilon$) acting opposite to the fin Magnus force. The distance l between these forces can be estimated assuming the Magnus force acts at the center of the fins so that the couple is

$$m_p = lN\sin\varepsilon = lN_p \tag{3}$$

Using the data of Fig. 2 and normal force and pitching moment data on this configuration obtained from F. Ragan in a private communication, it is possibe to determine ε, β, and $C_Y - C_n\sin\varepsilon$ for each angle of attack. Originally the author had just computed ε and β for the case where the pure couple was present (i.e., $\alpha = 6°$). During the review of this report, C. H. Murphy point out the possibility of doing this at each angle of attack, viz.,

$$C_Y = C_N\sin\varepsilon + C_{Np}(pd/u)\cos\varepsilon \tag{4}$$

and

$$C_n = l_N C_N\sin\varepsilon + l_F C_{Np}(pd/u)\cos\varepsilon \tag{5}$$

Above, it is assumed that the side force C_Y and the yawing moment C_n presented by Ragan are not divided by the spin. We write

$$\sin\varepsilon = (C_n - l_F C_Y)/[(l_N - l_F)C_N] = (C_n - l_F C_Y)/lC_N \tag{6}$$

For each angle of attack, Eq. (6) can be solved for ε by inserting the known values of C_n, C_Y and C_N while values of l and l_F can be estimated by assuming the Magnus force center of pressure is at the mid-chord of the fins. This can be done in this case for only the fins are rotating and creating the Magnus force. In the case of a finned projectile where the body rotates, l_F cannot be used.

For the data of Ref. 1 the values of β computed at each angle of attack ranged from 0.11° to 0.42°. For detailed computations of this correction see Ref. 2. This indicates that the variation of

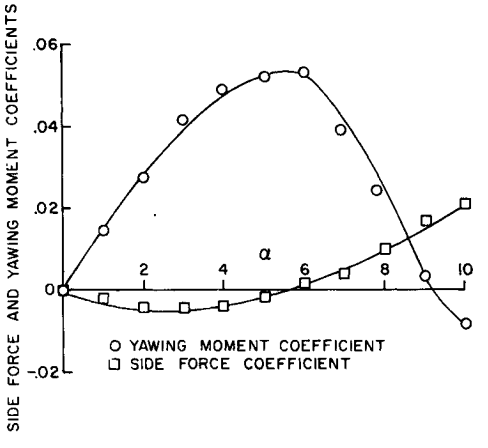

Fig. 2 Side force and yawing moment coefficients vs angle of attack for a 4° fin cant at Mach number 0.90, $Re = 1.5\times10^6$.

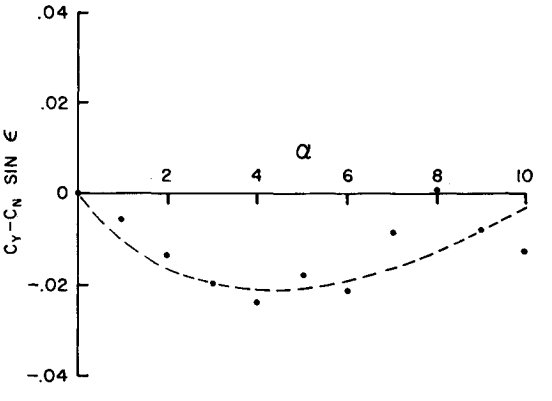

Fig. 3 Figure 2 corrected for normal force interaction.

flow inclination in the rest region is very good, but it also indicates that the normal force interaction term $N \sin \varepsilon$ is very sensitive to changes in β. Therefore, the computed correction may still contain errors of fairly high magnitude. A more exact way of obtaining accurate Magnus data is to obtain the side forces and moments at zero spin.

Conclusions

Wind-tunnel Magnus data obtained to date on canted fin configurations may be invalid in that a severe normal force interaction may be present. Although it may be possible in some cases to correct for this interaction, it is in general best to remove the interaction by subtracting the zero spin data at each angle of attack. This requires a system in which the model can be kept at zero spin during an angle of attack sweep of the configuration.

References

[1] Ragan, F. J., "Magnus Measurements on a Free Spinning Stabilizer," AIAA Paper 70-559, Tullahoma, Tenn., 1970.

[2] Platou, A. S., "Wind Tunnel Magnus Testing of a Canted Fin or Self-Rotating Configuration," Ballistic Research Labs., Memo Rept. 2143, AD No. 736369, Dec. 1971, U.S. Army Aberdeen Research and Development Center, Aberdeen Proving Ground, Md.

Determining the Nature of Instability in Nonconservative Problems

RAYMOND H. PLAUT*
Brown University, Providence, R.I.

Introduction

IN aeroelastic and other nonconservative problems, instability may occur either by divergence or flutter.[1] It is of practical interest to know which type of instability will occur; for example, if instability is of the divergence type a lower bound for the critical load often may be obtained.[2] In this Note a certain class of continuous elastic systems under nonconservative loading is considered. First, the slopes of the loading-frequency curves are determined, then necessary conditions for flutter and divergence instability are derived, and finally the application of these results to the determination of the nature of instability is discussed and an example is presented.

Analysis

Consider a system whose deflection modes $y_n(\mathbf{x})$ are governed by the differential equation

$$-\mu(\mathbf{x})\Omega_n y_n(\mathbf{x}) + \mathscr{E} y_n(\mathbf{x}) + P\mathscr{T} y_n(\mathbf{x}) = 0 \tag{1}$$

Received February 7, 1972; revision received March 15, 1972. This research was supported in part by the U.S. Army Research Office—Durham under Grant DA-31-124-ARO-D-270 and in part by the U.S. Navy under Grant NONR N00014-67-A-0191-0009. The author wishes to thank H. Leipholz of the University of Waterloo for several stimulating discussions on the topic.

Index category: Structural Stability Analysis.

* Assistant Professor of Applied Mathematics and Engineering (Research).

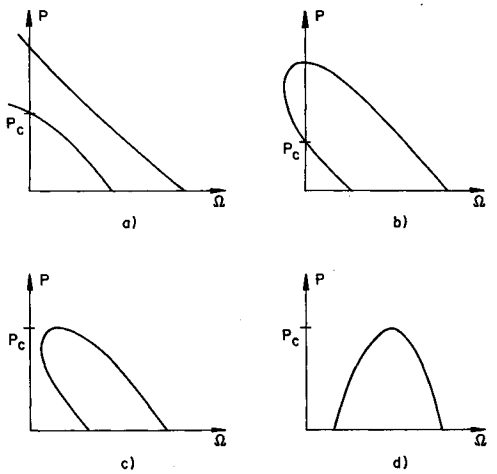

Fig. 1 Typical loading-frequency curves.

and the homogeneous boundary conditions

$$\mathscr{B} y_n(\mathbf{x}) = 0 \tag{2}$$

Here $P \geqq 0$ is the loading parameter, Ω_n is the frequency squared, $\mu(\mathbf{x}) > 0$ is the mass density, and $\mathscr{E}$, $\mathscr{T}$, and $\mathscr{B}$ are linear differential operators in terms of $\mathbf{x}$ and are independent of t and P. $\mathscr{E}$ is assumed to be self-adjoint and positive-definite. The stability of the equilibrium state $y_n(\mathbf{x}) \equiv 0$ is to be examined.

The condition for a nontrivial solution $y_n(\mathbf{x})$ of Eqs. (1) and (2) leads to a characteristic equation

$$F(\Omega_n, P) = 0. \tag{3}$$

Solution of Eq. (3) yields a loading-frequency relationship

$$P = p(\Omega_n) \tag{4}$$

Typical loading-frequency curves are shown in Fig. 1. At $P = 0$ the frequencies are real and positive and, assuming they are distinct, can be ordered by $0 < \Omega_1 < \Omega_2 < \ldots$. As P is increased the system may become unstable by divergence, as in Fig. 1 (a) and (b) at P_c, when one root Ω_n of Eq. (3) passes through zero to negative values, or by flutter, as in Fig. 1 (c) and (d) at P_c, when two roots merge and then become complex. Since Eq. (3) may be a complicated transcendental equation, it is useful to obtain some qualitative information on the properties of the loading-frequency curves.

The adjoint system to Eqs. (1) and (2) is defined by the equation

$$-\mu(\mathbf{x})\Omega_n z_n(\mathbf{x}) + \mathscr{E} z_n(\mathbf{x}) + P\mathscr{L} z_n(\mathbf{x}) = 0 \tag{5}$$

and boundary conditions

$$\mathscr{A} z_n(\mathbf{x}) = 0 \tag{6}$$

where the operators $\mathscr{L}$ and $\mathscr{A}$ are such that

$$\int z_n \mathscr{T} y_n \, d\mathbf{x} = \int y_n \mathscr{L} z_n \, d\mathbf{x} \tag{7}$$

whenever Eqs. (2) and (6) are satisfied. If Eq. (1) is multiplied by z_n and integrated over $\mathbf{x}$, one obtains

$$P = \left(\Omega_n \int \mu z_n y_n \, d\mathbf{x} - \int z_n \mathscr{E} y_n \, d\mathbf{x}\right) \Big/ \int z_n \mathscr{T} y_n \, d\mathbf{x} \tag{8}$$

This expression is stationary with respect to changes in y_n and z_n satisfying Eqs. (2) and (6), respectively. Differentiation thus yields the expression

$$dp/d\Omega_n = \int \mu z_n y_n \, d\mathbf{x} \Big/ \int z_n \mathscr{T} y_n \, d\mathbf{x} \tag{9}$$

for the slopes of the loading-frequency curves.

Substitution of Eq. (4) into Eq. (3) and differentiation of the resulting identity gives

$$\partial F/\partial \Omega_n + (\partial F/\partial P)\, dp/d\Omega_n = 0 \tag{10}$$

At a double root Ω_n the first term in Eq. (10) is zero, and assuming P is not concurrently a double root leads to